

High resolution SEM analysis of acellular glomerular basement membrane following pepsin digestion: intrinsic fibrillar structures

Walter J. Berger and Edward C. Carlson

Department of Anatomy and Cell Biology, School of Medicine, University of North Dakota, Grand Forks, North Dakota, USA

Summary. Microdissection of acellular rat renal cortex with pepsin was carried out to investigate the morphological substructure of glomerular basement membrane (GBM) by high resolution SEM. Renal cortical blocks ($< 5 \text{ mm}^3$) from adult male Sprague Dawley rats were rendered acellular by sequential detergent extraction and digested up to 184 hrs with 5 mg/ml pepsin (185 U/mg) in 0.5 M acetic acid (pH 2) at 10-15°C. Samples were conventionally prepared for SEM, and observed at original magnifications of 500-100,000 diameters.

At low magnifications (500-5,000x), acellular GBM surfaces appeared smooth at all digestion times. At higher magnifications (50,000-100,000x), control GBM surfaces were finely granular. Granule diameter ranged from 20-80 nm, with most between 30-40 nm. Pepsin digestion did not affect average granule size.

Beginning at 44 hrs of digestion, intrinsic fibrillar structures comprised of linear arrays of 20-40 nm granules were observed on/in GBM surfaces. At later incubation times, this component of GBM became more extensive. At 160 hrs, the fibrillar arrays frequently bifurcated and showed distinctive «forked» termini, some of which comprised two sides of a triangle (120-150 nm on a side). Fork «handles» (310-350 nm in length) radiated from each angle of the triangle. These sometimes terminated in large granules (approximately 100 nm in diameter), two of which appeared to connect fibrillar arrays end-to-end. Together with other arrays, the interconnected triangles appeared to comprise a three-dimensional meshwork extending into the GBM and possibly providing support for, its granular components.

Key words: Renal cortex, Glomerular basement membrane, Proteolytic digestion, Intrinsic fibrils

Introduction

The development by Crewe (1973) of a field emission source for electron microscopes provided the requisite characteristics of beam current, probe diameter, and resistance to spatial drift which, when applied to scanning electron microscopy (SEM), routinely provided a resolution close to the theoretical limit of 2 nm, and thus permitted high resolution observation of objects of macromolecular dimensions. More recently, modifications of standard SEM preparative techniques have been developed to optimize their use with biological specimens (Peters and Green, 1983; Peters, 1985, 1986a,b,c). By these methods investigations of macromolecular structures have been carried out by high resolution SEM (Peters et al., 1983, 1985).

High resolution SEM has only recently been utilized to examine substructural features of isolated or acellular basement membranes (BMs). Sawada (1981) used this technique to demonstrate acellular renal BM surfaces in mice and rats, and showed that, unlike their appearance at lower magnifications, BM surfaces were not smooth, but consisted of a «granular matrix». Likewise Ichimura and Hashimoto (1984) utilized, «freeze-cracking» of neuronal tissue to produce partially denuded BM surfaces allowing direct visualization of the components of basal lamina and lamina reticularis. The most extensive studies of BM ultrastructure utilizing high resolution SEM have been carried out by Carlson and co-workers who showed, following detergent treatment to remove cells, the detailed topography of major renal cortical BMs (Berger and Carlson, 1986, 1987) and retinal vessel BMs (Carlson, 1988, 1989, 1990; Carlson et al., 1988; Carlson, Carlson and Bjork, 1990) by SEM at original magnifications up to 100,000 diameters.

These studies have shown that it is possible by high

Offprint requests to: Edward C. Carlson, Department of Anatomy and Cell Biology, University of North Dakota, Grand Forks, ND 58202, USA

This work was done in partial fulfillment of the requirements for the degree of Doctor of Philosophy and was presented in preliminary form at the 100th meeting of the American Association of Anatomists, Washington, D.C., May 10-14, 1987.

SEM analysis of microdissected GBM

resolution SEM techniques to investigate BM surface morphology on the macromolecular scale. In this regard, considerable progress in understanding the structure and macromolecular organization of typical BMs has been made as a result of analyses of extracts of the «BM matrix»-producing Englebreth-Holm-Swarm (EHS) tumor (Orkin et al., 1977; Timpl et al., 1984). Several major components have been isolated, and individual molecules visualized utilizing rotary shadowing procedures (Timpl, 1985, 1986; Martin et al., 1985; Yurchenco et al., 1986; Martínez-Hernández, 1987).

Since the sizes of many molecular components of BM fall within the limits of resolution of current SEM technology (Timpl, 1986), and since their characteristic shapes are known, it seems reasonable to use this instrumentation to attempt to visualize molecules which comprise glomerular BMs (GBMs). However, studies by Sawada (1981) and by Carlson and co-workers (Berger and Carlson, 1987; Carlson, 1988, 1989, 1990; Carlson et al., 1988; Carlson and Bjork, 1990) indicate that acellular GBMs show homogeneous granular surfaces, and are devoid of the «amorphous feltwork...of fibrils» (Kefalides, 1971) traditionally described in high magnification transmission electron microscopic (TEM) studies. Moreover, the major BM glycoproteins isolated from the EHS tumor are best described as fibrillar (Orkin et al., 1977), and high resolution SEM studies of authentic BMs have not provided evidence for distinguishable fibrillar profiles.

Of the known BM components, the macromolecular shape and intramolecular interactions of type IV collagen are best understood. It is believed to form an extensive support meshwork for BMs (Timpl et al., 1981; Yurchenco et al., 1986; Inoue and LeBlond, 1988). A convenient characteristic of type IV collagen is that it is relatively resistant to pepsin degradation under conditions which conserve the integrity of helical regions (Kefalides, 1968). Accordingly, Carlson, et al. (1978a) demonstrated by TEM that pepsin digestion of isolated renal tubular BMs (TBMs) resulted in the release of striated collagen fibrils from the sample. More recently, human GBMs have been subjected to limited pepsin digestion resulting in the demonstration by TEM of a network of 3-8 nm intrinsic GBM fibrils and quasi-hexagonal crystalline structures (Carlson and Audette, 1989).

The purpose of the current investigation was to extend these studies to the level of high resolution of SEM using pepsin digestion of acellular renal cortical blocks in an effort to microdissect GBMs, and to demonstrate substructural features which can be related to their constituent macromolecules.

Materials and methods

Five adult male Sprague-Dawley rats (350-450 gm), were anesthetized with an intraperitoneal injection of 1 ml sodium pentobarbital (65 mg/ml), and the abdominal wall incised and reflected. The peritoneal cavity was

opened, the diaphragm punctured, and kidneys were collected. Renal capsules were removed, the cortex was «pinched off» with fine forceps, and minced into pieces approximately 2-4 mm³ (Cohen and Carlson, 1984). Cortical blocks were stored in 0.85% NaCl on ice until all kidneys were processed.

Cortical blocks were exposed to detergent-endonuclease treatment (Meezan et al., 1975; Carlson et al., 1978b), as modified by Carlson and Kenney (1980) to remove cells from tissue blocks. All solutions were prepared in distilled water which included 0.1% sodium azide, and the volume of each solution adjusted to 50-100X the wet weight of tissue samples. Tissue blocks were continuously agitated on an oscillating shaker, and washed extensively between solutions with distilled water.

After initial overnight immersion in 10mM ethylenediaminetetraacetic acid (EDTA), tissue blocks were sequentially exposed to 3% triton X-100 (12 hrs; 4°C), 0.025% deoxyribonuclease in 1M NaCl (6 hrs; 4°C), and 4% deoxycholate (25°C). After a final distilled water rinse, cortical blocks were stored in distilled water/azide at 4°C.

The protocol for pepsin digestion used to microdissect acellular renal GBMs prior to SEM was adapted from previous studies on isolated, acellular rabbit renal TBMs and GBMs by Carlson et al. (1981). Pilot experiments on acellular renal cortical blocks using 0.1% pepsin (185 U/mg) in 0.5 M acetic acid (pH 2, 4°C), with enzyme changed every four hours, exhibited minimal digestion at 12 hrs when evaluated by SEM. Accordingly, the experiments were repeated with 0.5% pepsin at 10-15°C for up to 184 hrs, with the enzyme changed as samples were collected for the first 72 hrs, then changed at eight hour intervals to the end of the experiment. Samples were collected at four hour intervals for the first 24 hrs, at six hour intervals for the next 48 hrs, and then at 88, 120, 160 and 184 hrs. Samples also included hour zero (fixed with no treatment) and acetic acid (treated as in pepsin experiments but without enzyme) controls. Immediately following removal from the enzyme, acellular tissues were washed three times in 25 mM tris-buffered saline (pH 7.6), then fixed and stored at 4°C.

Following initial fixation in Karnovsky's (1965) 0.2 M cacodylate-buffered paraformaldehyde/glutaraldehyde (4°C, pH 7.4, minimum 1 hr), tissues were rinsed in 0.1 N s-collidine buffer (pH 7.4) and post-fixed in collidine-buffered 1% OsO₄. Between rinses in distilled water, they were serially treated 60 min *en bloc* with collidine-buffered 1% tannic acid (Siomionescu and Simionescu, 1976) followed by 90 min in 1% aqueous uranyl acetate (Carlson and Hinds, 1981). All rinses were carried out at least three times beyond the point of clearing.

Acellular renal cortical blocks were dehydrated through a graded ethanol series, critical point dried in a Sam-Dri critical point dryer, mounted on aluminum specimen stubs, and coated with gold-palladium, on a Technics Hummer I sputter coater at 10 mA. To preserve relevant detail at high magnification, metal coating

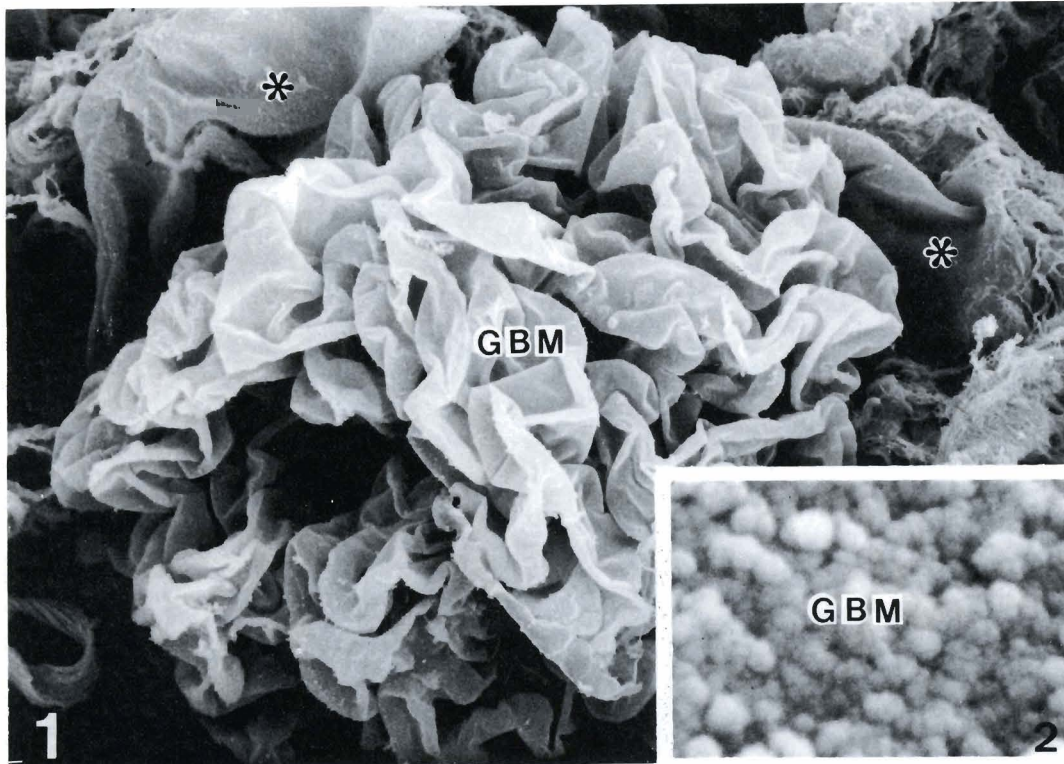


Fig. 1. Acellular glomerular basement membrane (GBM) appears as a tuft of anastomosing capillary channels. GBMs are 100-200 μm in diameter and surrounded by a «half-shell» of Bowman's capsule basement membrane (asterisks). $\times 1,500$



Fig. 2. At high magnification, glomerular basement membrane (GBM) external surfaces appear pebbled or granular. Granules are tightly-packed and range from 20-60 nm, with most > 40 nm. $\times 100,000$

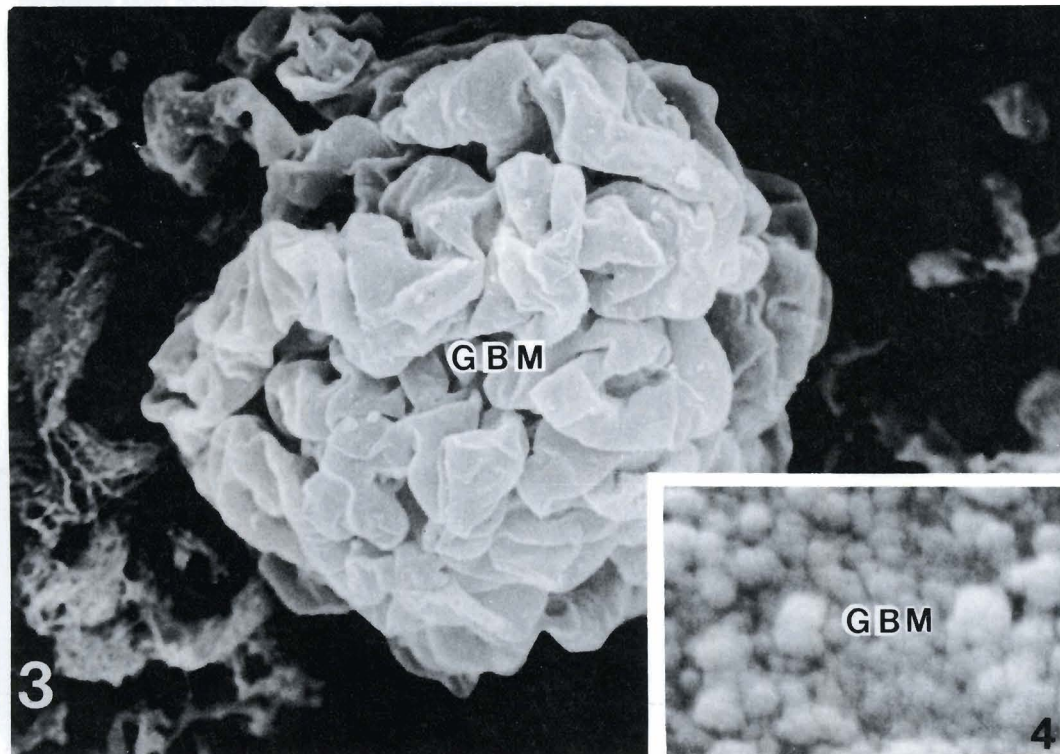


Fig. 3. After 184 hrs exposure to acetic acid alone, acellular glomerular basement membrane (GBM) is indistinguishable from controls. $\times 1,500$



Fig. 4. High resolution SEM shows glomerular basement membrane (GBM) external surfaces are not affected by extended exposure (148 hrs) to acetic acid. $\times 100,000$

thickness was minimized by coating for 2.5 min, repeating 0.5 min intervals until specimens displayed no charging during observation at accelerating voltages of 15-30 kv. Observations were carried out on a Hitachi S-800 field emission SEM, at original magnifications of 750-100,000 diameters.

Results

In onset control acellular renal cortical tissue blocks, GBMs (100-200 μm) are typically surrounded by a «half shell» of Bowman's capsule basement membrane (BCBM) that separates convoluted tufts of glomerular

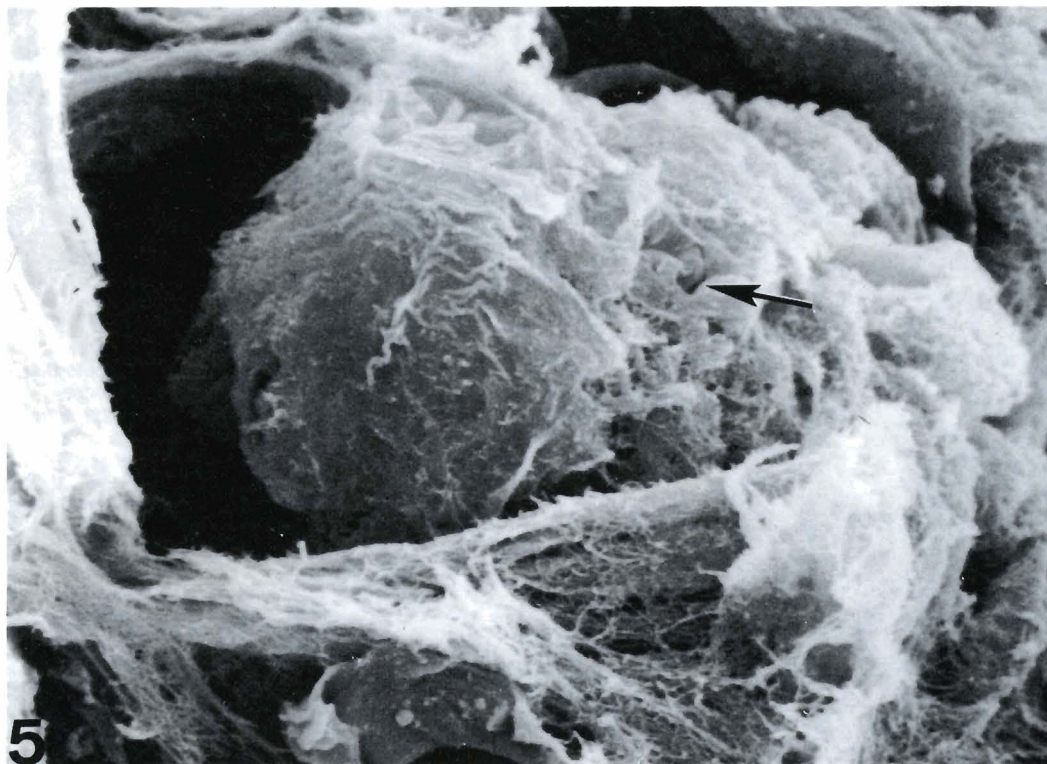


Fig. 5. Scanning electron micrograph of acellular renal cortex following 44 hrs pepsin digestion. Glomerular basement membrane capillary channels (arrow) are often obscured by partially-digested Bowman's capsule basement membrane. Arrow also indicates area of GBM shown at higher magnification in Fig. 6. $\times 1,250$

Fig. 6. Higher magnification of area at arrow in Fig. 5. Where GBM is not covered by partially digested fibrillar Bowman's capsule basement membrane, the fine granular glomerular basement membrane (GBM) texture is similar to controls (compare with Figs. 2, 4). $\times 30,000$

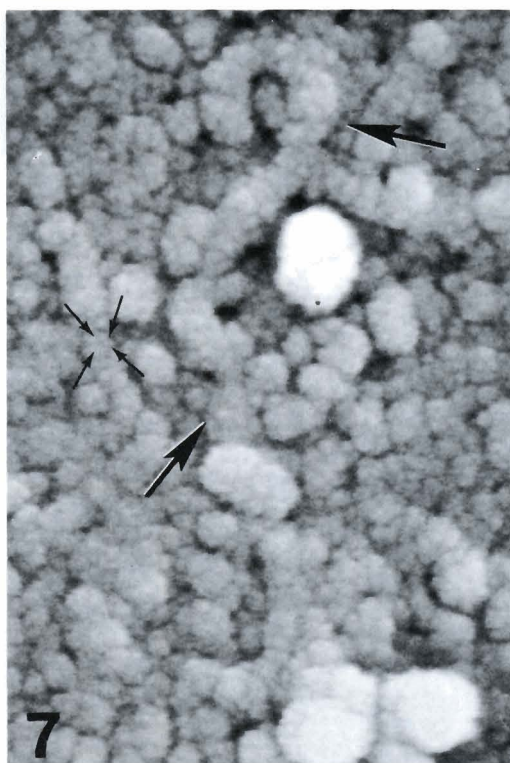
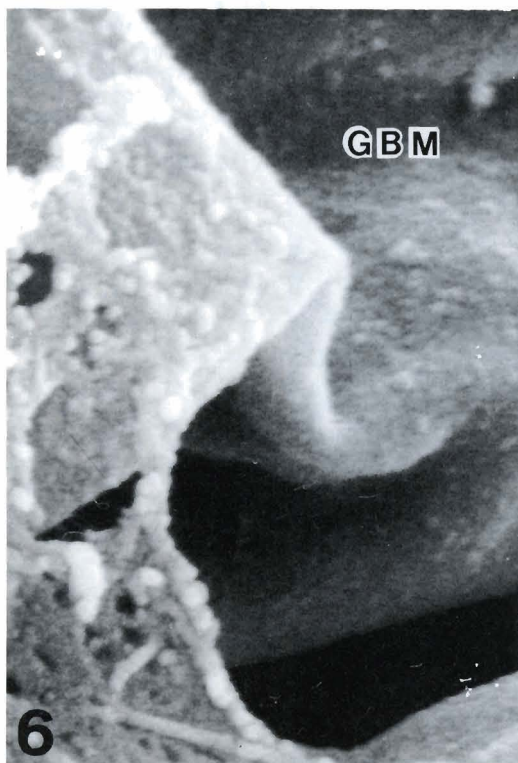


Fig. 7. Following 44 hrs pepsin digestion, high resolution SEM shows 40 nm fibrils or linear arrays of 20-40 nm granules (large arrows) appear to merge with external GBM surfaces. The smallest particles (approximately 5 nm; small arrows) may represent aggregates of gold-palladium conductive metal coat. $\times 100,000$

capillary BMs from the general renal cortical extracellular matrix (ECM; Fig. 1). Individual capillary loops frequently appear distended or partially collapsed. Unlike BCBMs and TBMs, GBMs are almost never sectioned during conventional preparation of cortical tissue blocks, so that only their external (epithelial) surfaces

are visible. By high resolution SEM (Fig. 2), GBM surfaces present a «pebbled» or granular appearance. Granules range from 20-80 nm, with most measuring less than 40 nm in diameter. Extended (184 hrs) treatment of tissue blocks with acetic acid alone produced no visible change in the appearance of GBMs when viewed by low

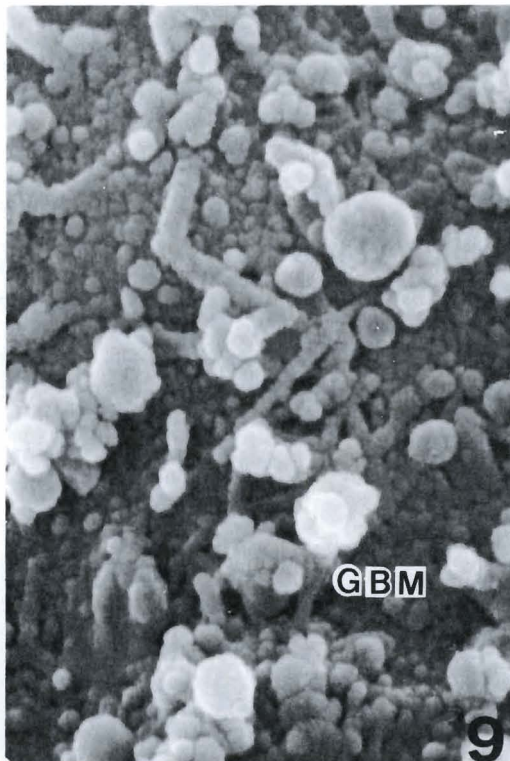
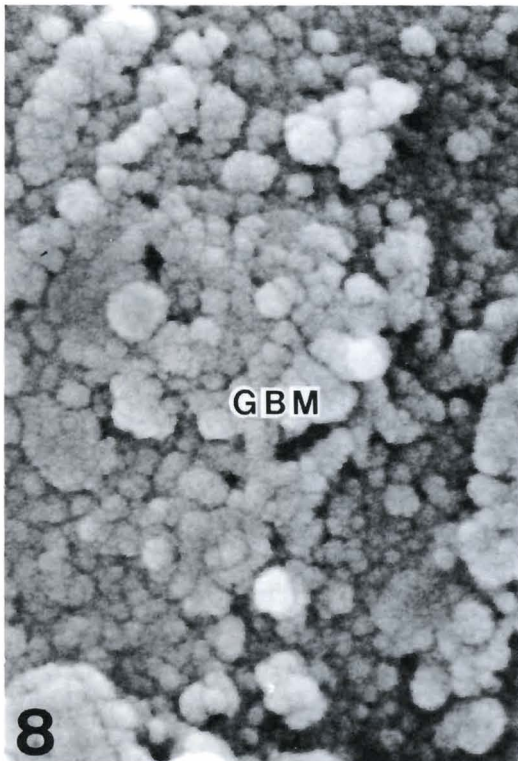


Fig. 8. Except for the large aggregates (which may represent «debris» typical of prolonged pepsin digestion), most GBM surfaces do not differ substantially from controls following 160 hrs pepsin digestion (compare with Figs. 2, 4). $\times 80,000$

Fig. 9. After 160 hrs pepsinization, SEM shows that fibrillar arrays are occasionally present on glomerular basement membrane (GBM) surfaces, but are often partially obscured by granular aggregates. $\times 30,000$

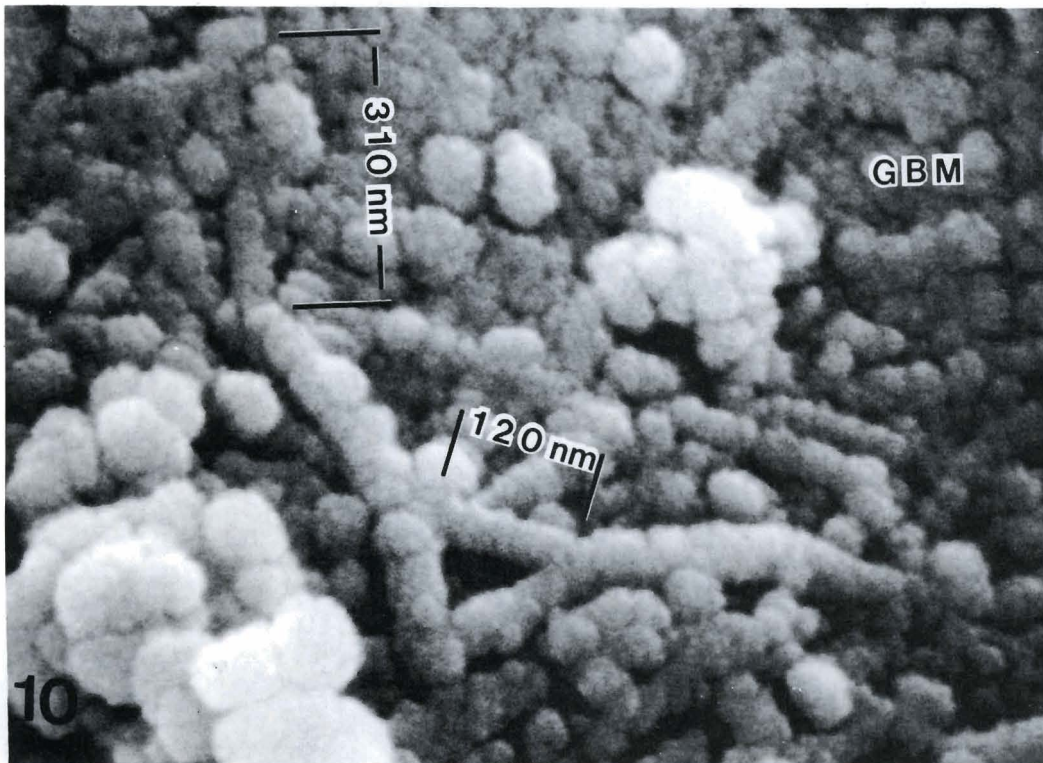


Fig. 10. Following 160 hrs of digestion, high resolution SEM shows 40-70 nm fibrils (linear arrays of granules) which appear integral to the glomerular basement membrane (GBM) matrix. In some areas, linear arrays join in a triangular pattern. $\times 100,000$

(Fig. 3) or high (Fig. 4) resolution SEM.

After 44 hrs of pepsin digestion, GBM surfaces often are obscured by overlying remnants of partially-digested BCBM (Fig. 5). Even at intermediate magnifications (Fig. 6), it is apparent that the compact pebbled texture of control GBMs is not substantially altered. However,

at higher magnifications, sinuous intrinsic fibrils or arrays of granules approximately 40 nm in diameter are occasionally visible, with ends embedded in the GBM surface (Fig. 7).

With extended pepsin digestion times, portions of GBM surfaces are often partially obscured by large gra-

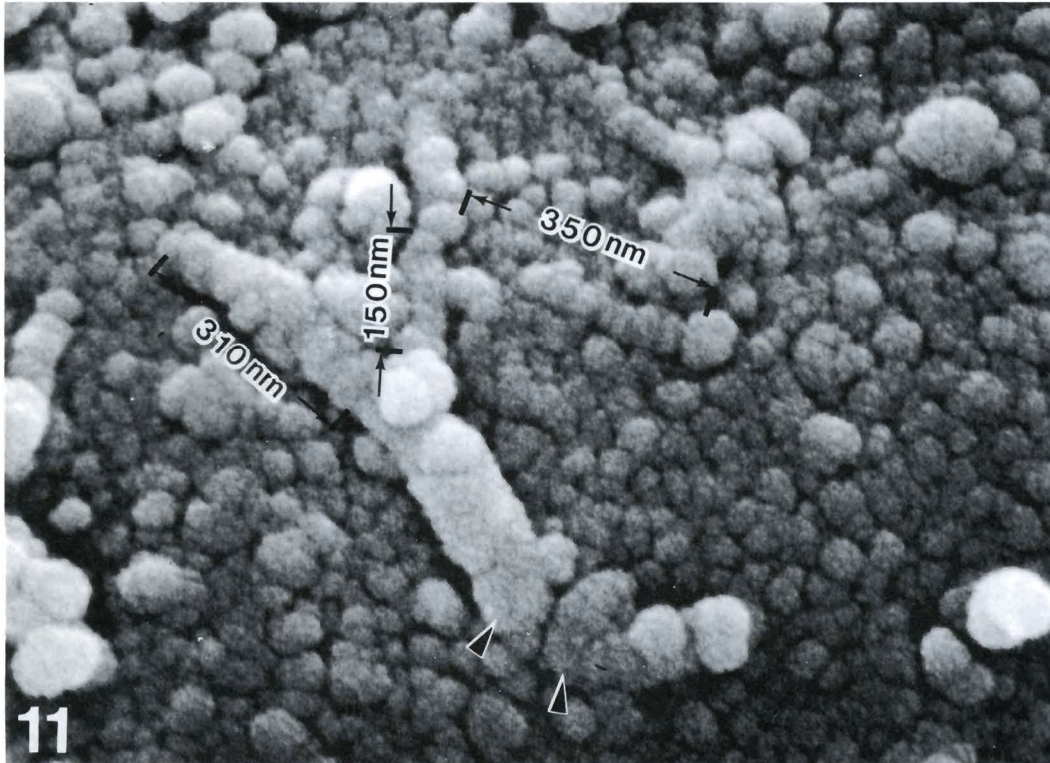


Fig. 11. High resolution SEM of glomerular basement membrane (GBM) external surfaces following 184 hrs pepsin digestion. Fibrillar arrays of granules are bifurcated, and also show interactions between terminal granules approximately 100 nm in diameter connecting arms in an array (arrowheads). $\times 100,000$

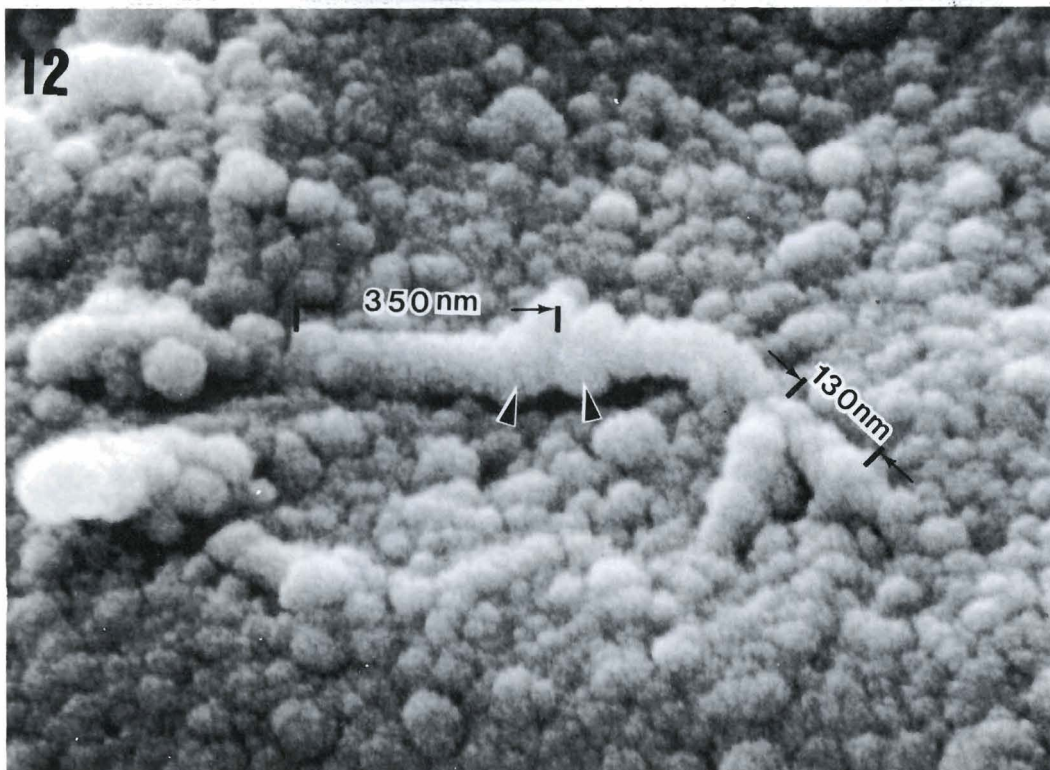


Fig. 12. Following 184 hrs of pepsin treatment, terminal granules (arrowhead) frequently interconnect. A fork-like fibrillar array extends to the right. $\times 100,000$

nular aggregates (Figs. 8-12). Since these aggregates also appear randomly on fibrils and BM surfaces at all pepsin digestion times and their amount is roughly proportional to the length of pepsin digestion, they may represent protease cleavage products incompletely cleared during washes.

Following 160 hrs of pepsin digestion, most GBM surfaces are ragged (Fig. 8), and the generally homogeneous appearance characteristic of controls is lost (compare Fig. 8 with Figs. 2 and 4). In many areas unrelated to large granular aggregates, linear fibrillar arrays of 40-70 nm granules are prominent (Fig. 9), and

merge with the substance of the GBM (Fig. 10). Moreover, these arrays frequently interconnect to form a branching meshwork of characteristic «forked» junctions with linear distances of 310-350 nm and 120-150 nm.

Similar fibrillar arrays of 40-70 nm granules are seen in GBMs following 184 hrs pepsin digestion. While it is not clear that substantially more digestion occurs at this time, patterns of arrays are more regular (Figs. 11, 12). As at 160 hrs, fibrillar arrays frequently exhibit forked termini; these and the included angle occasionally comprise two sides of a triangle measuring 120-150 nm on a side. A quasi-triangular network of arrays is thus formed, with fork «handles» (approximately 310-350 nm in length) radiating from the angles. These often terminate in large (approximately 100 nm) granules, two of which occasionally form end-to-end connections with other linear arrays (Fig. 12). Together, the arrays comprise a three-dimensional «meshwork» extending into the granular component of GBM.

Discussion

Two major morphological alterations of GBM granular matrix occur during pepsin digestion. Most apparent is the formation of large diameter (> 80 nm) granules and aggregates of 20-60 nm granules on all GBM surfaces, especially at the extremes of pepsin digestion. Although positive identification of the granules is not possible by current SEM techniques, it seems most likely that they represent hydrated domains of polysaccharide chains of proteoglycans, e.g. heparan sulfate proteoglycan (HSPG), and/or the associated carbohydrate side chains of glycoproteins such as type IV collagen and laminin (Berger and Carlson, 1986, 1987; Carlson, 1988). When Turley and co-workers (1985) combined known proteoglycans of extracellular matrix with collagen lattices to form artificial matrices it was noted that, while chondroitin sulfate proteoglycan precipitated on collagen fibrils as 27-37 granules, «free» chondroitin sulfate formed 100-200 nm spheres. Thus, the appearance of large diameter granules during pepsin digestion seen in the present study may be related to condensation of glycosaminoglycan side chains released by proteolysis. In addition, the large granular aggregates seen in the present study correlate quantitatively with increased pepsin digestion times and are present on all renal BM and ECM components. It seems possible therefore that the aggregates may represent contaminating «debris» rather than authentic GBM components unmasked during enzyme microdissection.

The second major alteration in the random pattern of granular GBM matrix is the appearance of intrinsic fibrils, or, more specifically, linear arrays of granules 40-70 nm in diameter. Sinuous fibrils which merge with the surrounding granular matrix are occasionally visible as early as 44 hrs of digestion. As pepsinization progresses, an extensive bifurcating fibrillar meshwork with distinctive forked termini, become apparent. Fork «handles» measure 310-350 nm, with «tines» measuring

120-150 nm. The interconnected linear arrays appear to form a polygonal, three-dimensional meshwork which could extend throughout, and possibly provide support for the granular component of the GBM.

Of the known components of BM, only type IV collagen is believed to form interconnecting polygonal arrays acting as a support for other BM components. Although the production of linear arrays in the current study by pepsin digestion does not result in an end-associated «chicken-wire» model, as proposed for type IV collagen (Timpl et al., 1981), or the more complex model of overlapping, laterally-associated collagen molecules (Yurchenco and Furthmayr, 1984), linear dimensions of fork «handles» approximate the length of one-half of a type IV dimer (320 nm; Laurie et al., 1981). Furthermore, the length of fork «tines» is similar to the overlap distance in irregular polygonal lattices observed by Yurchenco and Furthmayr (1984) when isolated type IV collagen molecules were allowed to reaggregate (approximately one-fifth the length of a dimer, or 130-170 nm, depending on the lattice model). In addition, the apparent joining of two linear arrays by large granules is reminiscent of the demonstrated end-association between type IV molecules by globular NC1 fragments (Timpl et al., 1981; Weber et al., 1984).

It must be pointed out that the diameter of the interconnected arrays described above is at variance with the diameter of molecules proposed by others to provide a supporting meshwork for GBM. Indeed, they are considerably larger than either the fibrillar components of BM as seen by TEM (3-8 nm; Inoue and LeBlond, 1983; Carlson and Audette, 1989) and type IV collagen molecules as seen by rotary shadowing (Timpl et al., 1981; Yurchenco and Furthmayr, 1984). At 40-70 nm in diameter, they represent one third the average thickness of rat GBM as determined by TEM. Accordingly, analogies between the linear arrays seen in the present study and the end-region associated model of type IV collagen interaction of Timpl et al. (1981) are problematic. Even alternative models proposing lateral associations require at least 13 parallel molecules to increase them to the minimum 40 nm diameter, while the most complex model (Yurchenco and Furthmayr, 1984) allows for only three collagen molecules per side.

The simplest explanation for the extreme diameter of the linear arrays is artifact due to excessive application of the conductive metal coats. For this to be the cause, however, coating thickness would necessarily approximate 20 nm. At that thickness, the coating would likely obliterate any perception of BM surface features (Peters, 1986b). An alternative possibility is that the granules which comprise the GBM matrix represent ectodomains of proteoglycans. Such an interpretation seems reasonable because the observed 20-60 nm range of granule sizes matches estimates of GBM and cell surface proteoglycans obtained by TEM, including studies using cationic dyes (20 nm; Kanwar and Farquhar, 1979a,b; Reale, 1983, 1985), deep-etch replicas of GBM (15-40 nm; Kubosawa and Condo, 1985), or rotary shadowed, deembedded ECM of cock's comb (30-60 nm; Cidadao and David-

Ferreira, 1986). The correlation between granule diameters seen in these latter investigations with diameters obtained by our high resolution SEM studies suggests that the conductive coating may not be responsible for the observed diameter of the linear arrays.

Several concepts of BM supramolecular assembly have been suggested recently which may help to explain the large diameters observed in our study. Using immunostaining techniques, Laurie et al. (1984) showed that, in GBM, all known BM components colocalize to an anastomosing network of cords up to 10 nm in diameter. Considering the possible organization of components of these cords, Inoue and LeBlond (1988) have suggested that laminin, nidogen, and fibronectin might associate laterally with axial type IV collagen molecules to form elongate bundles. Similarly, the comprehensive model of BM supramolecular structure of Yurchenco et al. (1986), incorporates nidogen/laminin, HSPG/laminin, and HSPG/type IV collagen interactions which could contribute to larger diameter structural units.

Although the largest cords seen by Laurie et al. (1984) are 10 nm in diameter, heavy metals used in TEM to enhance specimen contrast delineate polysaccharides poorly compared to lipids and proteins. Thus, the measured diameter of the cords may reflect predominantly cores of fibrillar proteins. If the granular appearance of BM seen in SEM reflects the image of space-filling hydrated ectodomains of HSPG side chains, it would require only a single layer of 20-30 nm granules surrounding a 4 nm cord to generate a 40-70 nm diameter structure similar to the linear arrays seen in this study.

In summary, pepsin digestion of acellular rat GBM gives indications of a substructure consonant with current concepts of BM supramolecular structure. Fibrils or more specifically, linear arrays of granules 40-70 nm in diameter, appear to form an interconnecting meshwork merging into the surrounding granular matrix. Though no unambiguous identification of known BM components is currently possible by SEM techniques, our study demonstrates that high resolution SEM of protease-digested GBM provides new information regarding its supramolecular organization and structure.

Acknowledgements. Thanks are extended to Faye Aker who typed the manuscript. The work was supported in part by a NSF/EPSCOR Grant R118610675 and a Grant from the American Diabetes Association, North Dakota Affiliate, Inc.

References

- Berger W.J. (1987). Basement membrane heterogeneity: A high resolution SEM study of renal basement membrane ultrastructure following enzyme microdissection. University of North Dakota.
- Berger W.J. and Carlson E.C. (1986). High resolution SEM of acellular renal basement membranes following streptomyces griseus protease (SGP) dissection. *Anat. Rec.* 214, 11a.
- Berger W.J. and Carlson E.C. (1987). A high resolution SEM analysis of acellular glomerular basement membrane following pepsin digestion. *Anat. Rec.* 218, 16a.
- Carlson E.C. (1988). Topographical specificity in isolated retinal capillary basement membranes: a high-resolution scanning electron microscope analysis. *Microvasc. Res.* 35, 221-235.
- Carlson E.C. (1989). Fenestrated subendothelial basement membranes in human retinal capillaries. *Invest. Ophthalmol. Vis. Sci.* 30, 1923-1932.
- Carlson E.C. 1990. Human retinal capillary basement membrane leaflets are morphologically distinct: a correlated TEM and SEM analysis. *Exp. Eye Res.* (in press).
- Carlson E.C. and Bjork N.J. (1990). SEM and TEM analysis of isolated human retinal microvessel basement membranes in diabetic retinopathy. *Anat. Rec.* (in press).
- Carlson E.C. and Audette L. (1989). Intrinsic fibrillar components of human glomerular basement membranes: a TEM analysis following proteolytic dissection. *J. Submicrosc. Cytol. Pathol.* 21, 83-92.
- Carlson E.C. and Hinds D. (1981). Native banded collagen fibrils in the glomerular mesangial matrix of normal human and laboratory animals. *J. Ultrastruct. Res.* 77, 241-247.
- Carlson E.C. and Kenney M.C. (1980). Morphological heterogeneity of isolated renal basement membranes. *Renal Physiol.* 3, 288-297.
- Carlson E.C. and Kenney M.C. (1982). An ultrastructural analysis of isolated basement membranes in the acellular renal cortex: a comparative study of human and laboratory animals. *J. Morphol.* 171, 195-211.
- Carlson E.C., Brendel K., Meezan E. (1978a). Striated collagen fibrils derived from ultrastructurally pure isolated basal lamina. In: *Biology and chemistry of basement membranes*. Kefalides N.A. (ed) Academic Press. New York. pp 31-41.
- Carlson E.C., Brendel K., Hjelle J.T. and Meezan E. (1978b). Ultrastructural and biochemical analyses of isolated basement membranes from kidney glomeruli and tubules and brain and retinal microvessels. *J. Ultrastruct. Res.* 62, 26-53.
- Carlson E.C., Meezan E., Brendel K. and Kenney M.C. (1981). Ultrastructural analyses of control and enzyme treated isolated renal basement membranes. *Anat. Rec.* 200, 421-436.
- Cidadao A.J. and David-Ferreira J.F. (1986). A method for TEM visualization of the extracellular matrix three-dimensional organization in tissues. *J. Microsc.* 142, 49-62.
- Cohen M.P. and Carlson E.C. (1984). Preparation and analysis of glomerular basement membrane. In: *Methods of diabetes research*. Larner J. and Pohl S.L. (eds). Vol. 1. Laboratory Methods. Pt. C. John Wiley and Sons. New York. pp 357-375.
- Crewe A.V. (1973). Production of electron probes using a field emission source. In: *Progress in optics XI*. Wolf E. (ed). North-Holland Publishing Co. Amsterdam. pp 225-248.
- Inoue S., LeBlond C.P. and Laurie G.W. (1983). Ultrastructure of Reichert's membrane, a multilayered basement membrane in the parietal wall of the rat yolk sac. *J. Cell Biol.* 97, 1524-1537.
- Inoue S. and LeBlond C.P. (1988). Three-dimensional network of cords: the main component of basement membranes. *Am. J. Anat.* 181, 341-358.
- Kanwar Y.S. and Farquhar M.G. (1979a). Anionic sites in the glomerular basement membrane. *J. Cell Biol.* 81, 137-153.

- Kanwar Y.S. and Farquhar M.G. (1979b). Isolation of glycosaminoglycans (Heparan Sulfate) from Glomerular basement membranes. *Proc. Natl. Acad. Sci., U.S.A.*, 76, 4493-4497.
- Karnovsky M.J. (1965). A formaldehyde-glutaraldehyde fixative of high osmolality for use in electron microscopy. *J. Cell Biol.* 27, 137a-138a.
- Kefalides N.A. (1968). Isolation and characterization of the collagen from glomerular basement membrane. *Biochemistry* 7, 3103-3112.
- Kefalides N.A. (1971). Isolation and characterization of cyanogen bromide peptides from basement membrane collagen. *Biochem. Biophys. Res. Commun.* 47, 1151-1158.
- Kubosawa H. and Kondo Y. (1985). Ultrastructural organization of the glomerular basement membrane as revealed by a deep-etch replica method. *Cell Tissue Res.* 242, 33-39.
- Laurie G.W., LeBlond C.P., Inoue S., Martin G.R. and Chung A. (1984). Fine structure of the glomerular basement membrane and immunolocalization of five basement membrane components to the lamina densa (Basal Lamina) and its extensions in both glomeruli and tubules of the rat kidney. *Am. J. Anat.* 169, 463-481.
- Martin G.R., Timpl R., Muller P.K. and Kuhn K. (1985). The genetically distinct collagens. *Trends Biochem. Sci.* 10, 285-287.
- Martínez-Hernández A. (1987). Electron immunohistochemistry of the extracellular matrix: an overview. In: *Methods in enzymology*. Cunningham L. (ed). Vol. 145, *Structural and Contractile Proteins. Part E, Extracellular Matrix*. Academic Press. Orlando, pp 78-103.
- Meezan E., Hjelle J.T., Brendel K. and Carlson E.C. (1975). A simple, versatile, nondisruptive method for the isolation of morphologically and chemically pure basement membranes from several tissues. *Life Sci.* 17, 1721-1732.
- Orkin R.W., Gehron P., McGoodwin E.B., Martin G.R., Valentine T. and Swarm R.J. (1977). A murine tumor producing a matrix of basement membrane. *J. Exp. Med.* 145, 204-220.
- Peters K.-R. (1985). Working at higher magnifications in scanning electron microscopy with secondary and backscattered electrons on metal coated biological specimens and imaging macromolecular cell membrane structures. *Scan. Electron Microsc.* 4, 1519-1544.
- Peters K.-R. (1986a). High magnification scanning electron microscopy. *J. Electron Microsc. Tech.* 4, 102-113.
- Peters K.-R. (1986b). Metal deposition for high magnification electron microscopy. In: *Advanced techniques in biological electron microscopy III*. Koehler J.K. (ed). Springer-Verlag. New York. pp 1-62.
- Peters K.-R. (1986c). Rationale for the application of thin, continuous metal films in high magnification electron microscopy. *J. Microscopy* 142, 25-34.
- Peters K.-R. and Green S.A. (1983). Macromolecular structures of biological specimens are not obscured by controlled osmium impregnation. 41st Ann. Proc. E.M.S.A. pp 606-607.
- Peters K.-R., Palade G.E., Schneider B.G. and Papermaster D.S. (1983). Fine structure of a periciliary ridge complex of frog retinal rod cells revealed by ultrahigh resolution scanning electron microscopy. *J. Cell Biol.* 96, 265-276.
- Peters K.-R., Carley W.W. and Palade G.E. (1985). Endothelial plasmalemmal vesicles have a characteristic striped bipolar surface structure. *J. Cell Biol.* 101, 2233-2238.
- Reale E., Luciano L. and Kuhn K.W. (1983). Ultrastructural architecture of proteoglycans in the glomerular basement membrane: a cytochemical approach. *J. Histochem. Cytochem.* 31, 662-668.
- Reale E., Luciano L. and Kuhn K.W. (1985). Cationic dyes reveal proteoglycans on the surface of epithelial and endothelial kidney cells. *Histochemistry* 82, 513-518.
- Sawada H. (1981). Structural variety of basement membranes: a scanning electron microscopic study. *Biomed. Res.* 2, 125-128.
- Simionescu N. and Simionescu M. (1976). Galloylglycoses of low molecular weight as mordant in electron microscopy. I. Procedure, and evidence for mordanting effect. *J. Cell Biol.* 70, 608-621.
- Timpl R. (1986). Recent advances in the biochemistry of glomerular basement membrane. *Kidney Int.* 30, 292-298.
- Timpl R., Fujiwara S., Dziadek M., Aumailly M., Weber S. and Engel J. (1984). Laminin, Proteoglycan, Nidogen and Collagen IV: Structural models and molecular interactions. *C.I.B.A. Fndn. Symp.* 108, 25-37.
- Turley E.A., Erickson C.A. and Tucker R.P. (1985). The retention and ultrastructural appearance of various extracellular matrix molecules incorporated into three-dimensional hydrated collagen lattices. *Dev. Biol.* 109, 347-369.
- Weber S., Engel J., Wiedemann H., Glanville R.W. and Timpl R. (1984). Subunit structure and assembly of the globular domain of basement membrane collagen type IV. *Eur. J. Biochem.* 139, 401-410.
- Yurchenco P.D. and Furthmayr H. (1984). Self-assembly of basement membrane collagen. *Biochemistry* 23, 1839-1850.
- Yurchenco P.D., Tsilibary E.C., Charonis A.S. and Furthmayr H. (1986). Models for the self-assembly of basement membrane. *J. Histochem. Cytochem.* 34, 93-102.

Accepted January 9, 1990